

# Hydrogen-Bonded Hybrid Multilayers: Film Architecture Controls Release of Macromolecules

Irem Erel-Unal and Svetlana A. Sukhishvili\*

Department of Chemistry, Chemical Biology and Biomedical Engineering, Stevens Institute of Technology, Hoboken, New Jersey 07030

Received June 16, 2008; Revised Manuscript Received September 15, 2008

**ABSTRACT:** We report on the construction of purely hydrogen-bonded hybrid polymer multilayers, which are composed of polymer pairs with low- and high- pH stability, and show that the critical pH value of film deconstruction, fraction of components released, and the rate of film dissolution can be tuned in a wide pH range from 3 to 9.5 by varying film composition and architecture. The film building blocks were poly(*N*-vinylcaprolactam) (PVCL)/poly(L-aspartic acid) (PLAA) bilayers as pairs of hydrogen-bonded polymers with low pH stability (critical disintegration pH of  $\sim 3.3$ ), and poly(*N*-vinylcaprolactam) (PVCL)/tannic acid (TA) bilayers as hydrogen-bonded polymers with a higher critical disintegration pH of  $\sim 9.5$ . Hybrid TA/PVCL/PLAA multilayers were prepared at low pH using a layer-by-layer technique. Film deposition and pH-induced deconstruction were followed by *in situ* Fourier transform infrared spectroscopy in attenuated total reflection mode (ATR-FTIR) and phase-modulated ellipsometry. PVCL/TA and PVCL/PLAA pairs were deposited in either alternating or stacked manner. Films with various layer arrangements had drastically different pH dissolution profiles. In all cases, the presence of PVCL/TA layers shifted pH values for release of PLAA from the film to more basic values. In the films with stacked architecture [(PVCL/PLAA)<sub>6</sub>(PVCL/TA)<sub>*n*</sub>], the mode of film destruction was dependent on both the amount of consecutively deposited PVCL/PLAA pairs and the number of PVCL/TA layer pairs in the surface stack. For the films composed of six bilayers of PVCL/PLAA in the base stack, the critical pH for film disintegration and PLAA release varied with the thickness of the top (PVCL/TA)<sub>*n*</sub> stack in a range from pH 3.5 to 5 with *n* ranging from 0 to 12. In hybrid alternating films, [(PVCL/TA)<sub>1</sub>(PVCL/PLAA)<sub>1</sub>]<sub>*n*</sub> (1:1), release of PLAA and TA was more interdependent. The proximity of PVCL/TA pairs has further delayed PLAA release up to near-neutral pH. In addition, PLAA chains diffusing through the film triggered disruption of PVCL/TA interactions resulting in release of  $\sim 15$ –20% of TA. These results demonstrate the effects of proximity and intermixing of hydrogen-bonded polymer pairs of greatly different pH stability on film decomposition modes. The possibility of releasing active molecules and/or polymers combined with the biocompatibility of film components makes such systems attractive candidates for future biomedical applications.

## Introduction

Incorporation of weakly acidic or basic polyelectrolytes (“weak polyelectrolytes”) within electrostatically assembled layer-by-layer (LbL) films has been of specific interest as properties of these films such as film thickness, morphology and wettability can be tuned by simple adjustment of the pH and/or ionic strength of the assembly and/or postassembly solutions.<sup>1–5</sup> Weak polyelectrolyte multilayers (wPEMs) have been recently suggested for use as antireflection coatings,<sup>6</sup> films for pH- and/or T-triggered loading and release of dyes or drugs,<sup>7,8</sup> films that control electroosmotic flow in microchannels,<sup>9</sup> or as matrices for fabrication of novel metal-containing inorganic nanocomposite materials.<sup>10,11</sup> While many research groups rely on electrostatic pairing between polyacids and polybases during fabrication of PEMs, hydrogen-bonding was also introduced as an alternative route to produce LbL films.<sup>12,13</sup> This approach was widened by one of us by demonstrating the erasability of hydrogen-bonded films of polycarboxylic acids and neutral polymers via pH variations.<sup>14</sup>

Hybrid layers of electrostatically assembled wPEMs have been earlier constructed and used for selective decomposition of one of the polyelectrolyte pairs in solutions with high concentrations of salts. Specifically, Schlenoff et al. reported on formation of free-standing poly(styrene sulfonate) (PSS)/poly(diallyldimethylammonium chloride) PDADMA membranes using salt-induced selective dissociation of poly(acrylic acid) (PAA)/PDADMA substrate stacks within hybrid [PAA/PDAD-

MA]<sub>*n*</sub> [PSS/PDADMA]<sub>*m*</sub> films.<sup>15</sup> In the same paper, the use of pH has also been reported to selectively decompose a substrate multilayer stack of PSS/PAA-PDADMA copolymer to yield a free-standing PSS/PDADMA film. Caruso and co-workers were first to fabricate hybrid wPEM films composed of both hydrogen-bonded and electrostatically assembled layers. They exploited the pH-triggered erasability of hydrogen-bonded polymer stacks sandwiched between electrostatically bound layers to selectively decompose such hybrid films to yield free-standing membranes of electrostatically assembled polymer pairs.<sup>16</sup>

Another motivation for constructing hybrid multilayers is to control chain exchange and release of functional molecules from PEMs. First, it recently became obvious that chain exchange and interdiffusion may occur within multilayers during film deposition or after exposure to solutions of different polyelectrolytes at the postself-assembly step. For example, Schaaf’s group showed that macromolecules such as poly(L-glutamic acid) and hyaluronic acid can diffuse in and out of a multilayer film during the deposition cycle.<sup>17,18</sup> These studies involved oligomeric molecules with  $\alpha$ -helical or  $\beta$ -sheet conformations. For the case of linear polyelectrolytes, Sui and Schlenoff considered the mobility of polyelectrolyte chains within wPEM films while describing pH-triggered polyelectrolyte charge extrusion to the surface of wPEM films,<sup>19</sup> and directly demonstrated the existence of such an exchange between wPEMs and solution using hydrogenated and deuterated polycarboxylic acids.<sup>20</sup> More recently, Hammond et al. reported on exchange of polybases between wPEMs and the solution,<sup>21</sup> and also showed that diffusion of polymer in/from multilayer films was

\* Corresponding author.

strongly dependent on the polycation charge density.<sup>22</sup> One strategy to control sometimes unwanted interdiffusion of chains within a film is to constrain interdiffusing polymer layers within the film by depositing stacks of strongly associated polymers. Such a barrier layer approach was pursued by Lavalle and co-workers in order to compartmentalize exponentially grown hyaluronic acid/poly(L-lysine) layers using poly(styrene sulfonate)/poly(allylamine) stacks.<sup>23</sup>

Electrostatically assembled hybrid multilayers can also be used to control the delivery rate of biologically active molecules. Hammond and co-workers studied drug release properties of films composed of alternately deposited hydrolytically degradable poly( $\beta$ -amino ester) and therapeutic polysaccharides, and found that film degradation and release was pH-dependent and followed pseudofirst order kinetics.<sup>24,25</sup> To achieve time-extended release kinetics, these authors constructed electrostatically assembled hybrid films, and covalently cross-linked stacks of barrier layers to block interlayer diffusion within the film.<sup>26</sup>

Here, we report on purely hydrogen-bonded hybrid films, composed of components with drastically different pH-dissociation properties, and explore the role of film architecture on pH-triggered release of film constituents. This study is built on our recent finding that critical dissolution pH values for film decomposition are drastically increased when neutral polymers are self-assembled with a polyphenol (tannic acid). Varying the nature of neutral polymers and/or ionic strength of the post-treatment solution, we were able to extend the critical disintegration pH range of tannic acid multilayers from neutral to basic conditions.<sup>27</sup>

In this paper, we constructed hydrogen-bonded hybrid multilayers using polymer pairs which decomposed at acidic (PVCL/PLAA) and basic (PVCL/TA) pH values, and explore how mutual arrangement of these polymer pairs within the film affects the mode of release of different film components. Taking advantage of ATR-FTIR spectroscopy we showed that, in the case of alternating TA/PVCL/PLAA films, selective release of PLAA occurs at near-neutral pH values and this is followed by dissolution of remaining PVCL/TA under basic conditions. Significantly, release of PLAA from alternating TA/PVCL/PLAA films was extended by 3–4 pH units to more basic conditions compared to PVCL/PLAA films. For stacked hybrid layers, we found that easily ionizable PVCL/PLAA pairs can serve as release layers for PVCL/TA stacks, and such systems can be used for pH-triggered fabrication of free-standing membranes. Therefore, we demonstrate that film dissolution and release of individual components can be efficiently controlled in purely hydrogen-bonded films by constructing hybrid multilayers.

## Experimental Section

**Materials.** Poly(*N*-vinylcaprolactam) (PVCL;  $M_w$  1800) was purchased from Polymer Source, Inc. Tannic acid (TA;  $M_w$  1701.20), poly(L-aspartic acid) sodium salt (PLAA;  $M_w$  15 000–50 000), hydrochloric acid, sodium hydroxide, monobasic sodium phosphate, dibasic sodium phosphate were purchased from Sigma-Aldrich. D<sub>2</sub>O with 99.9% isotope content was purchased from Cambridge Isotope Laboratories. All chemicals were used as received. Deionized (DI) water was purified using a Milli-Q system (Millipore).

**Deposition of Multilayers for Ellipsometry Measurements.** Multilayers of PVCL/PLAA or PVCL/TA were deposited at the surface of oxidized silicon wafers from 0.5 mg/mL polymer solutions in 0.01 M phosphate buffer at pH 2. Prior to film deposition, silicon wafers were irradiated with UV light for 2 h followed by rinsing with DI water and treating with concentrated sulfuric acid for 10 min. After rinsing with DI water, silicon wafers were immersed in 0.25 M NaOH solution for 10 min, rinsed with DI water and dried with nitrogen gas. The reason for treating silicon wafers with concentrated sulfuric acid and NaOH was to create

high density of silanol groups at the surface of silicon wafers. The latter is essential for the deposition of hydrogen-bonded films, whose precursor-free deposition relied on adhesion of the first polymer layer to the substrate via hydrogen-bonding interactions between surface silanol groups and carbonyl groups of a neutral polymer.

Film depositions were performed by immersing the silicon wafers in polymer solutions for 5 min followed by two intermediate rinsing steps with 0.01 M phosphate buffer at pH 2. All films were deposited using a Catalyst 3 Robot Arm (CRS Robotics Corp.) operated with homemade software. Film thickness was measured using a homemade phase-modulated ellipsometer.<sup>28</sup> pH-triggered destruction of the films was investigated by exposing the films to buffer solutions of increasing pH and subsequent drying followed by thickness measurements. Refractive index for ellipsometry measurements was fixed at 1.5. pH values of the buffer solutions were adjusted with HCl or NaOH solutions.

**Deposition of Multilayers for ATR-FTIR Measurements.** A Bruker Equinox-55 FTIR spectrometer equipped with a narrow-band mercury cadmium telluride detector and a home-built flow-through cell was used for *in situ* ATR-FTIR experiments. Multilayers were deposited on the surface of an oxidized silicon crystal installed within the flow-through stainless steel cell. Prior to film deposition, the silicon crystal was cleaned in the same way as described for silicon wafers in the previous section. PVCL, TA and PLAA were allowed to adsorb from 0.5 mg/mL solutions in buffered D<sub>2</sub>O at pH 2. This was followed by a rinsing step with 0.01 M phosphate buffer at pH 2. Layers were deposited without a precursor layer starting from PVCL, which adsorbed at the surface due to hydrophobic interactions, as well as due to hydrogen-bonding between carbonyl groups of PVCL and the silanol groups on the oxidized silicon wafer. pH-triggered destruction experiments were performed by sequentially filling the cell with buffered D<sub>2</sub>O at a specific pH value.

## Results and Discussion

We have shown earlier that the use of a water-soluble polyphenol, TA, in combination with neutral polymers, enables construction of hydrogen-bonded films with high pH-stability.<sup>27</sup> Different from earlier reported decomposition of neutral polymer/polycarboxylic acid films, neutral polymer/TA films did not dissolve at basic conditions.<sup>29</sup> However, dissolution of hydrogen-bonded films at neutral pH is a desirable property for releasing active molecules embedded within the film. We hypothesized that combining the polymer pairs of a neutral polymer and highly acidic PLAA, with the polymer pairs of a neutral polymer and low acidic TA, might result in modulation of the critical disintegration pH of hybrid films. Prior to fabrication of TA/PVCL/PLAA hybrid films, we investigated self-assembly and pH-stability of two-component neutral polymer/PLAA multilayer films.

**I. Hydrogen-Bonded PLAA/Neutral Polymer Films.** We found that at pH 2, PLAA could be self-assembled within LbL films with PVCL, but not with PVPON. Despite the similarity in chemical structure of PVCL and PVPON, the presence of two more methylene groups in the caprolactam ring contributed significantly to the hydrophobicity of PVCL and resulted in stabilization of hydrogen-bonded self-assembly.<sup>30</sup> PVCL/PLAA films showed a linear growth profile with a bilayer thickness of 10.1 nm (5.4 nm per PLAA and 4.7 nm per PVCL layer) when averaged over 11 bilayers starting from the fourth layer (Figure 1A).

At a deposition pH of 2, carboxylic groups of PLAA ( $pK_a = 3.53$ )<sup>31</sup> are mostly protonated, and PLAA is less than ~10% ionized when bound with PVCL (as will be shown below in Figure 2B). Therefore, association of PLAA chains with PVCL is primarily driven by hydrogen-bonding interactions between the carbonyl groups of PVCL and hydroxyl groups of the protonated carboxylic acids of PLAA (Scheme 1). Figure 1B

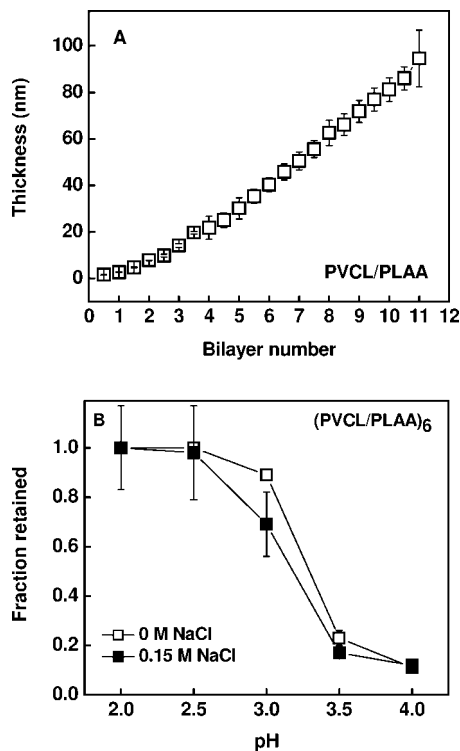


**Figure 1.** Ellipsometry data on LbL deposition of PVCL/PLAA at pH 2. Films were dried after each deposition step (panel A). pH-triggered disintegration of a 6-bilayer PVCL/PLAA film deposited at pH 2 and exposed to  $10^{-2}$  M phosphate buffer solutions of increasing pH with no additional salt (open squares) or 0.15 M NaCl (filled squares). Equilibrated values of fractions retained at the surface are plotted as a function of pH (panel B).

shows that as external pH was increased, PVCL/PLAA films dissolved because of enhanced ionization of PLAA and disruption of interpolymer hydrogen bonds. The critical disintegration pH, at which 50% of the film dissolved after equilibration time was  $\sim 3.3$  and correlated well with the  $pK_a$  of the polyacid of  $\sim 3.5$ . In 0.15 M NaCl solutions, films dissolved at a slightly lower pH, as high concentration of salt ions increased the ionization degree of PLAA. Importantly, dissolution of PVCL/PLAA films occurred at a much lower pH value than PVCL/TA films, which had a critical disintegration pH of 9.5.<sup>27</sup> In the next section, we combine the two types of hydrogen-bonded systems within hybrid films, and explored how the internal arrangement of pairs of hydrogen-bonded polymers affected film response to pH variations.

**II. Hybrid Hydrogen-Bonded TA/PVCL/PLAA Films.** In hybrid TA/PVCL/PLAA films, PVCL was used as a polymer capable of hydrogen-bonding with both TA and PLAA at low pH values. Scheme 2 illustrates that such binding can occur through hydrogen-bonding of carbonyl groups of the PVCL ring with phenolic hydroxyl groups of TA or hydroxyl groups of the protonated carboxylic acids of PLAA.

To study deposition and destruction of TA/PVCL/PLAA hybrid films, we have mostly used an *in situ* ATR-FTIR technique. The reason for this choice is the capability of this technique to selectively distinguish functional groups of film components. We were specifically interested in exploring mutual effects of PVCL/TA and PVCL/PLAA pairs on pH-triggered release of individual polymer components from the film.

Figure 2 shows representative ATR-FTIR spectra for (PVCL/TA)<sub>2</sub> (Figure 2A), (PVCL/PLAA)<sub>1</sub> (Figure 2B) and [(PVCL/TA)<sub>1</sub>(PVCL/PLAA)<sub>1</sub>]<sub>5.5</sub> (Figure 2C) films deposited at pH 2. For the (PVCL/TA)<sub>2</sub> films, three major bands are observed in the region from 1500 to 2000  $\text{cm}^{-1}$ : an absorption band at 1716

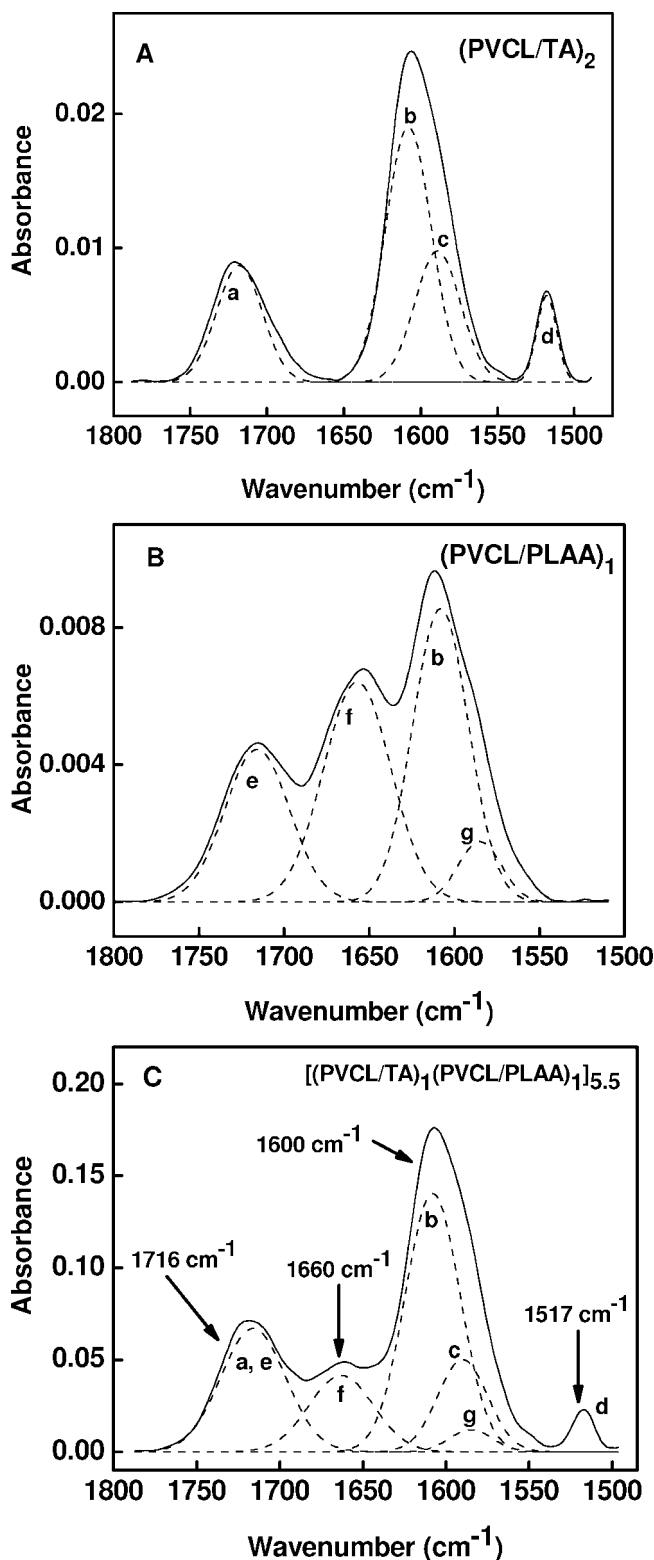
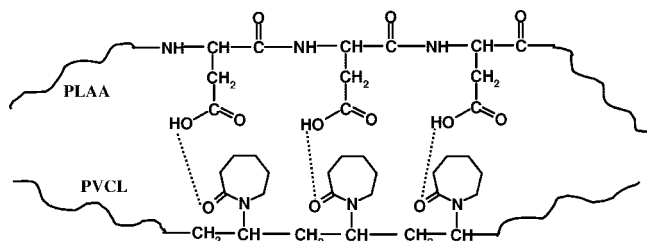


**Figure 2.** Representative ATR-FTIR spectra of (PVCL/TA)<sub>2</sub> (panel A), (PVCL/PLAA)<sub>1</sub> (panel B) and [(PVCL/TA)<sub>1</sub>(PVCL/PLAA)<sub>1</sub>]<sub>5.5</sub> (panel C) films. The measurements were done in D<sub>2</sub>O solution using 0.01 M phosphate buffer at pH 2. Letters correspond to the peak assignments indicated in the text.

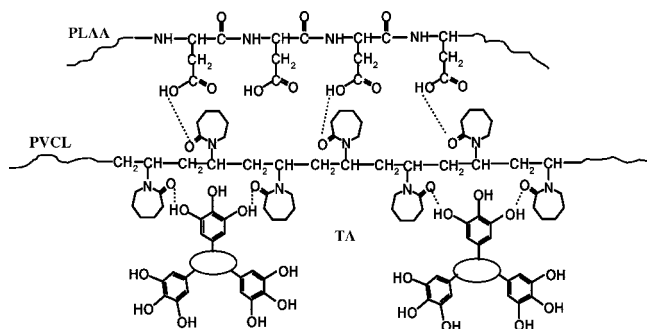
$\text{cm}^{-1}$  associated with stretching carbonyl vibrations of the TA ester groups (a); a strong absorption band at  $\sim 1600$   $\text{cm}^{-1}$  corresponding to carbonyl stretching vibrations of the caprolactam ring (b), which overlaps with stretching carbon-carbon vibrations of aromatic rings in TA (c), and a band at 1517  $\text{cm}^{-1}$  also associated with stretching vibrations of aromatic rings in



**Scheme 1. Schematic Representation of Hydrogen-Bonding Interactions between Carbonyl Groups of PVCL and Hydroxyl Groups of the Protonated Carboxylic Acids of PLAA**



**Scheme 2. Schematic Representation of Hydrogen-Bonding Interactions within TA/PVCL/PLAA Hybrid Films**



TA (d). (PVCL/PLAA)<sub>1</sub> films also exhibits three bands (Figure 2B): a peak at 1716 cm<sup>-1</sup> assigned to protonated carboxylic groups of PLAA (e); a band at 1660 cm<sup>-1</sup> originating from carbonyl stretching vibrations of  $\alpha$ -helical motifs of PLAA<sup>32</sup> (f); and a third band where carbonyl stretching 1600 cm<sup>-1</sup> vibrations of the caprolactam ring (b) overlaps with the COO<sup>-</sup> asymmetric stretching vibrational band of PLAA (g). Figure 2B shows that at deposition pH of 2 which is moderately lower than the pK<sub>a</sub> of ~3.53 for PLAA, PLAA in PVCL/PLAA films is partially ionized (an estimated value of ionization is less than 10%). Obviously, the known suppression of polyacid ionization due to hydrogen bonding with proton-accepting neutral polymers<sup>33</sup> was not very strong for the PVCL/PLAA pair. As a comparison, LbL films of poly(methacrylic acid) (PMAA) with PVCL were stable up to pH 6.95,<sup>30</sup> which is higher than the pK<sub>a</sub> of 6 for PMAA,<sup>34</sup> and at this point PMAA was 30% ionized. Inefficient suppression of ionization of carboxylic groups in PVCL/PLAA films is probably due to the helicity of PLAA, whose structural rigidity reduces the number of hydrogen bonds between PVCL and PLAA.

Figure 2C illustrates the spectrum for an alternating [(PVCL/TA)<sub>1</sub>(PVCL/PLAA)<sub>1</sub>]<sub>5.5</sub> hybrid film in the spectral range from 1500 to 2000 cm<sup>-1</sup>. The curve-fitting file created with the parameters obtained from individual spectra of film components did not result in reliable data analysis due to spectral overlap within the bands centered at 1716 and 1600 cm<sup>-1</sup>. However, the PLAA band at 1660 cm<sup>-1</sup> (f) could be clearly separated using curve-fitting to follow PLAA release. Also, for the pH range when three of the components are present within the film, we have used the total intensity of the ATR-FTIR spectra in the region from 1540–1770 cm<sup>-1</sup> to monitor pH-triggered film dissolution.

A simplified curve-fitting prepared to separate the absorbances of broad bands centered at 1600, 1660, and 1716 cm<sup>-1</sup> is shown in the Supporting Information, Figure 1S and Table 1S. At high pH values, when PLAA was completely released from the film, we were able to quantify the film components (the intensity of peak e was zero, and the whole intensity of the 1716 cm<sup>-1</sup> band could be related to the amount of TA). In addition, in selected

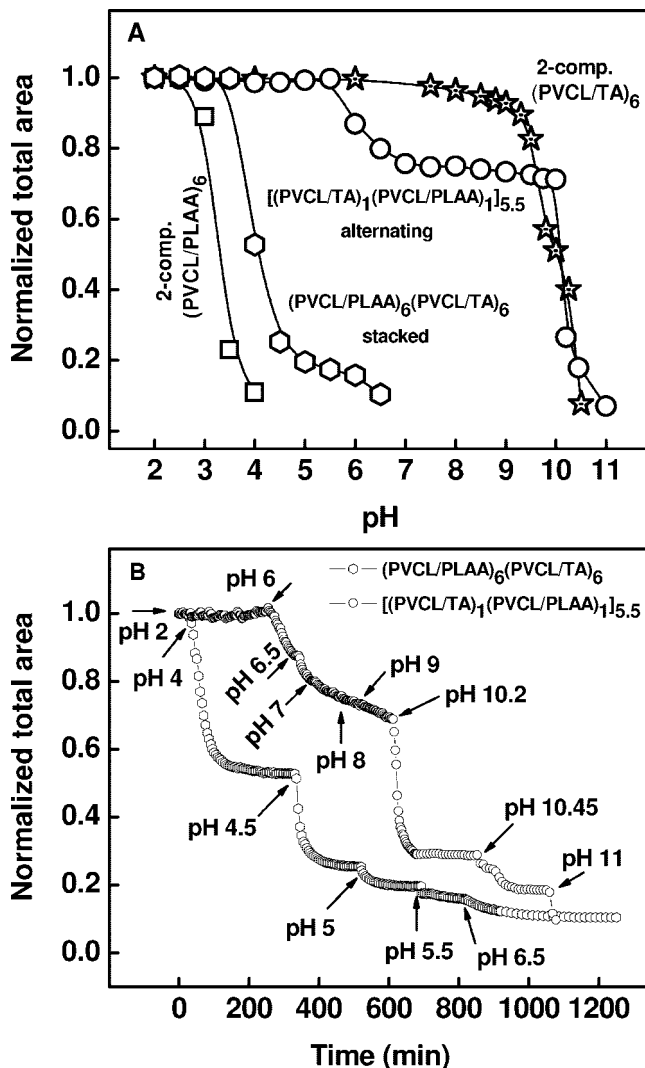


**Figure 3.** Equilibrated values (panel A) and kinetics (panel B) of pH-triggered disintegration of stacked (PVCL/PLAA)<sub>6</sub>(PVCL/TA)<sub>6</sub> (hexagons) and alternating [(PVCL/TA)<sub>1</sub>(PVCL/PLAA)<sub>1</sub>]<sub>5.5</sub> films (circles), deposited at pH 2 in 0.01 M buffered D<sub>2</sub>O and exposed to increasing pH. Film dissolution profiles for two-component (PVCL/PLAA)<sub>6</sub> (squares) and (PVCL/TA)<sub>6</sub> (stars) systems are also shown in panel A for comparison. Normalized total area in the 1540–1770 cm<sup>-1</sup> region is plotted as a function of either pH or time.

experiments we also monitored film thickness using ellipsometry. In general, total FTIR absorbance of overlapping bands in the region from 1540–1770 cm<sup>-1</sup> cannot be used to directly infer the amount of polymer deposited at the surface without knowing the extinction coefficients. However, normalized total absorbance and thickness obtained from ATR-FTIR and ellipsometry were consistent within 10% (see Supporting Information, Table 2S). This indicates that the mismatch of the extinction coefficients for various functional groups was moderate and did not significantly contribute to quantitative conclusions drawn in the paper.

**II.1. Alternating versus Stacked Films.** We have built films with PVCL/PLAA and PVCL/TA pairs which were variously arranged within the film, and explored the effect of film architecture on film decomposition when such films were exposed to solutions with increasing pH. Figure 3A shows pH dependence of the total absorbances of films in the 1540–1770 cm<sup>-1</sup> region (intensities were normalized to the total absorbance of assembled films at pH 2) for alternating [(PVCL/TA)<sub>1</sub>(PVCL/PLAA)<sub>1</sub>]<sub>5.5</sub> and (PVCL/PLAA)<sub>6</sub>(PVCL/TA)<sub>6</sub> stacked films. These hybrid multilayers included the same fraction of each

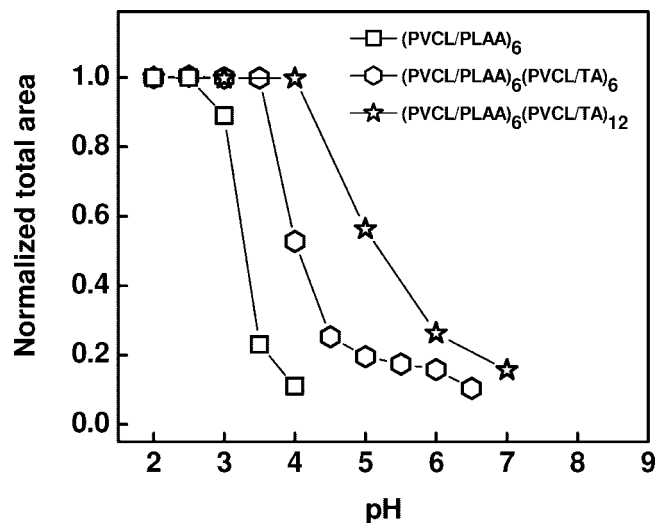


**Figure 4.** pH-triggered disintegration of (PVCL/PLAA)<sub>6</sub> (squares), (PVCL/PLAA)<sub>6</sub>(PVCL/TA)<sub>6</sub> stacked (hexagons), and (PVCL/PLAA)<sub>6</sub>(PVCL/TA)<sub>12</sub> stacked (stars) films, deposited at pH 2 and exposed to 0.01 M buffered D<sub>2</sub>O solutions of increasing pH. Normalized total area in the 1540–1770 cm<sup>-1</sup> region is plotted as a function of pH.

polymer component and differed only in their architecture. The destruction profiles for two-component PVCL/TA and PVCL/PLAA films are also plotted as a reference. Figure 3A illustrates the drastic effect of multilayer architecture on film deconstruction. While the onset of (PVCL/PLAA)<sub>6</sub>(PVCL/TA)<sub>6</sub> stacked film dissolution occurred at pH 4 which was only one unit higher than that for (PVCL/PLAA)<sub>6</sub> films, in the case of alternating hybrid film, mass loss did not occur until pH 6. (PVCL/PLAA)<sub>6</sub>(PVCL/TA)<sub>6</sub> stacked film completely deconstructed in a narrow pH range of 4–5, whereas the [(PVCL/TA)<sub>1</sub>(PVCL/PLAA)<sub>1</sub>]<sub>5.5</sub> alternating multilayer showed a distinct two-step release profile. Below, we will propose mechanisms for dissolution of stacked and alternating films.

**II.1.1. Dissolution Mechanism for Stacked Films.** In the case of stacked layers, the mechanism of film destruction involved not only direct electrostatic repulsions between charged carboxylic groups of PLAA, but to a large extent, the osmotic pressure of counterions which penetrate into the film to compensate excess charge on PLAA chains. Increased osmotic pressure causes diffusion of water into the film and results in swelling of the (PVCL/PLAA)<sub>6</sub> stack. When the osmotic pressure built within (PVCL/PLAA)<sub>6</sub> is no longer counterbalanced by the mechanical strength of the top PVCL/TA barrier layer, complete dissociation of PVCL/PLAA films occur. Figure 4 shows that with an increase in thickness of the stack layer, the critical dissolution pH of the films (and, correspondingly, pH for PLAA release) systematically shifted to higher pH values. The critical pH values were 3.3, 4 and 5 for (PVCL/PLAA)<sub>6</sub>, (PVCL/PLAA)<sub>6</sub>(PVCL/TA)<sub>6</sub> and (PVCL/PLAA)<sub>6</sub>(PVCL/TA)<sub>12</sub> films, respectively. For all stacked multilayers, the pH stability transition was sharp once the critical pH was achieved.

The effect of osmotic pressure on the complete dissociation of the multilayers following internal ionization has also been discussed by others. Sukhorukov et al. demonstrated that the hollow microcapsules composed of poly(allylamine hydrochloride) (PAH) and PMAA can swell and dissolve at low pH due to protonation of carboxylic acid groups resulting in uncompensated positive charges on PAH and an increase in osmotic pressure.<sup>35</sup> Schlenoff et al. also considered the effects of both electrostatic repulsion between excess charge and/or increased osmotic pressure in pH-triggered dissociation of multilayers containing a weak polyacid.<sup>36</sup>

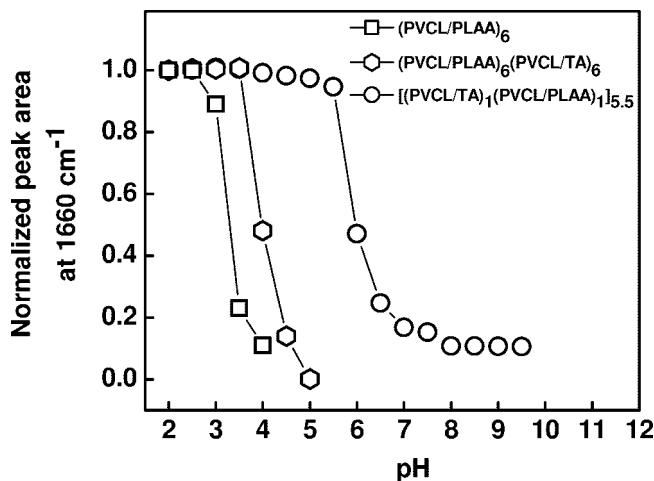


**Figure 5.** pH evolution of the normalized area of 1660 cm<sup>-1</sup> PLAA band in (PVCL/PLAA)<sub>6</sub>; (PVCL/PLAA)<sub>6</sub>(PVCL/TA)<sub>6</sub> stacked and [(PVCL/TA)<sub>1</sub>(PVCL/PLAA)<sub>1</sub>]<sub>5.5</sub> alternating films.

**II.1.2. Dissolution Mechanism for Alternating Films.** [(PVCL/TA)<sub>1</sub>(PVCL/PLAA)<sub>1</sub>]<sub>5.5</sub> alternating film showed a distinct two-step release profile: about 23% of film mass loss occurred at pH 6–7, while the rest of the film remained stable till pH 10.2. Final dissolution of the film occurred at pH ~10.2 which is very close to the previously reported critical disintegration pH of 9.5 for two-component PVCL/TA system determined using ellipsometry.<sup>27</sup> A small difference in the critical disintegration pH values can be attributed to isotopic effect, as in this study we used D<sub>2</sub>O instead of H<sub>2</sub>O. Taking advantage of the curve fitting of the ATR-FTIR intensities (see Supporting Information, Figure 1S), we show that the first step in film loss (pH region 6 to 7) for TA/PVCL/PLAA alternating multilayer films corresponded to a release of 90% of PLAA from the film (Figure 5). The remaining 10% of PLAA was probably included in several polymer layers close to the substrate surface, in which PLAA chains were entangled with other polymers and pinned to the substrate through adsorption of the first PVCL layer. Figures 3A and 5 show that while (PVCL/PLAA)<sub>6</sub>(PVCL/TA)<sub>6</sub> stacked films decomposed with release of the top PVCL/TA from the surface, [(PVCL/TA)<sub>1</sub>(PVCL/PLAA)<sub>1</sub>]<sub>5.5</sub> alternating film retained most of its mass (TA+PVCL) after removal of PLAA from the film. This is consistent with trends found for decomposition of purely electrostatic and hydrogen bonded/electrostatic hybrid films.<sup>15,16</sup>

Surprisingly, release of PLAA from [(PVCL/TA)<sub>1</sub>(PVCL/PLAA)<sub>1</sub>]<sub>5.5</sub> alternating films was drastically delayed from pH 3 to 6 as compared to PVCL/PLAA films. In the case of hydrogen-bonded/electrostatic hybrid films, Caruso reported a much smaller pH shift in film decomposition.<sup>16</sup> One possible reason for such a delay might be attributed to formation of hydrogen bonds between PLAA and TA within the film, however we found no evidence of association between PLAA and TA in solution. Importantly, using ATR-FTIR, we were able to conclude that ionization degree of PLAA at the critical pH for film destruction was drastically different from a 2-component (PVCL/PLAA)<sub>6</sub> film. The estimated ionization degree for [(PVCL/TA)<sub>1</sub>(PVCL/PLAA)<sub>1</sub>]<sub>5.5</sub> alternating film was 18 ± 3% and 55 ± 5% at pH 3.5 and pH 6, respectively.

We suggest that higher PLAA ionization tolerated by hybrid films compared to the two-component PVCL/PLAA system resulted from a “dilution” of PLAA charge by neighboring neutral PVCL and TA molecules. Such “dilution” is possible because of known fuzziness of polyelectrolyte multilayers,<sup>37</sup> in which polymer layers are highly diffused and interpenetrated. Assuming film density of 1 g/cm<sup>3</sup>, an average charge-to-charge

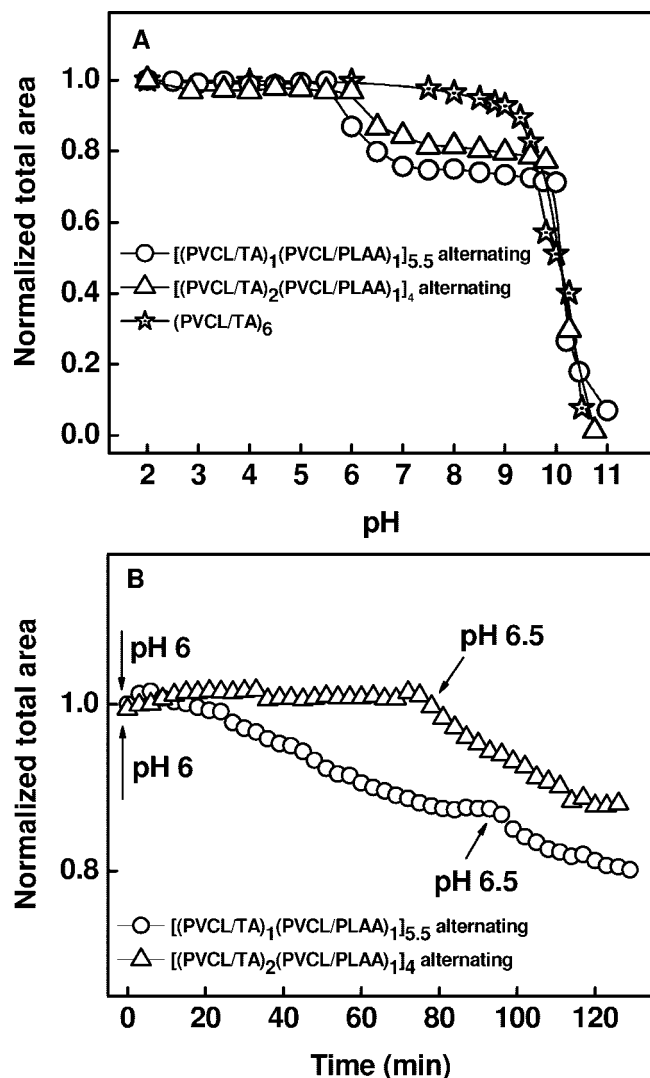


**Figure 6.** pH-triggered disintegration of [(PVCL/TA)<sub>1</sub>(PVCL/PLAA)<sub>1</sub>]<sub>5.5</sub> (circles) and [(PVCL/TA)<sub>2</sub>(PVCL/PLAA)<sub>1</sub>]<sub>4</sub> (triangles) alternating films deposited at pH 2 in 0.01 M buffered D<sub>2</sub>O. Film dissolution profiles for two-component PVCL/TA film (stars) are plotted for comparison (panel A). Kinetics of film deconstruction for both alternating TA/PVCL/PLAA multilayers at pH 6 and 6.5 (panel B).

distance between ionized groups of PLAA at critical dissolution pH can be estimated from the layer thicknesses of 5.4 nm (per PLAA layer) and 4.7 nm (per PVCL layer), and the thickness for PVCL/TA bilayer of ~4.6 nm.<sup>27</sup> Such an estimate leads to an average interchange spacing of  $11 \pm 1$  Å for the (PVCL/PLAA)<sub>6</sub> film, and of  $10 \pm 1$  Å for [(PVCL/TA)<sub>1</sub>(PVCL/PLAA)<sub>1</sub>]<sub>5.5</sub> alternating multilayer. These two values are close to one another, and illustrate the feasibility of the suggestion that volume charge density controls film destruction.

**Effect of Number of PVCL/TA Pairs in Alternating Films on Film Dissolution.** To further understand the effect of volume charge density on critical disintegration pH, we produced hybrid films in which every PVCL/PLAA bilayer is sandwiched between 2 bilayers of PVCL/TA, [(PVCL/TA)<sub>2</sub>(PVCL/PLAA)<sub>1</sub>]<sub>4</sub> (2:1). Figure 6A shows the normalized total area as a function of pH for [(PVCL/TA)<sub>1</sub>(PVCL/PLAA)<sub>1</sub>]<sub>5.5</sub> and [(PVCL/TA)<sub>2</sub>(PVCL/PLAA)<sub>1</sub>]<sub>4</sub> alternating hybrid multilayers. As seen in Figure 6A, both alternating systems exhibited a two-step disintegration profile. [(PVCL/TA)<sub>2</sub>(PVCL/PLAA)<sub>1</sub>]<sub>4</sub> alternating film retained PLAA up to a slightly higher pH value. In the case of [(PVCL/TA)<sub>1</sub>(PVCL/PLAA)<sub>1</sub>]<sub>5.5</sub> alternating system, selective release of PLAA chains occurred at pH 6, while [(PVCL/TA)<sub>2</sub>(PVCL/PLAA)<sub>1</sub>]<sub>4</sub> alternating system toler-

ated the ionization of PLAA until pH 6.5. This difference can be explained by the strong interpenetration of polymer layers within TA/PVCL/PLAA alternating films. We argue that alternating a bilayer of PVCL/PLAA after every two bilayers of PVCL/TA rather than one reduced local bulk charge density of PLAA and delayed its release to a higher pH value.

This difference in pH stability is also evident in kinetic experiments as shown in Figure 6B. At pH 6–7, where all film loss occurred due to diffusion of dissociated PLAA chains through PVCL/TA matrix, dissolution kinetics were slow, at the time scale of hours for both systems. Slow kinetics associated with diffusion of PLAA through PVCL/TA film are also illustrated for the whole pH range in Figure 3B. Considering PLAA as a model of polypeptide drug, these results show the possibility of tuning PLAA release to a higher pH value by increasing the number of highly pH stable PVCL/TA layers within the film.

Scheme 3 illustrates that the events following the disruption of PVCL/PLAA binding are drastically different for differently structured hybrid TA/PVCL/PLAA films. We believe that in the case of [(PVCL/TA)<sub>1</sub>(PVCL/PLAA)<sub>1</sub>]<sub>5.5</sub> alternating film, dissociation of PLAA from PVCL chains is followed by slow diffusion of free PLAA chains through the remaining polymer film (Scheme 3A), while in (PVCL/PLAA)<sub>6</sub>(PVCL/TA)<sub>6</sub> stacked films, such diffusion is inhibited due to complete dissolution of the PVCL/PLAA bottom stack and subsequent release of PVCL/TA layers from the surface (Scheme 3B).

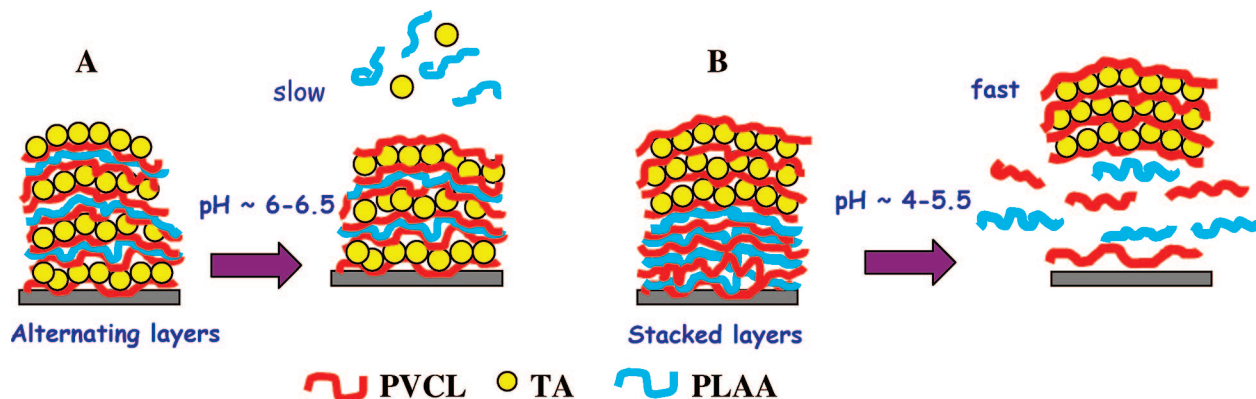
**II.2. Sandwiched TA/PVCL/PLAA Films.** We have also explored the effect of the number of PVCL/PLAA bilayers sandwiched between PVCL/TA stacks on pH-triggered film deconstruction. Figure 7 contrasts film disintegration for (PVCL/TA)<sub>4</sub>(PVCL/PLAA)<sub>2</sub>(PVCL/TA)<sub>4</sub> and (PVCL/TA)<sub>4</sub>(PVCL/PLAA)<sub>4</sub>(PVCL/TA)<sub>4</sub> multilayers. The destruction profile of a [(PVCL/TA)<sub>1</sub>(PVCL/PLAA)<sub>1</sub>]<sub>5.5</sub> alternating film is also shown for comparison.

As compared to the alternating multilayer system, the film loss at near-neutral pH reflecting PLAA release from the film is shifted progressively to lower pH values for (PVCL/TA)<sub>4</sub>(PVCL/PLAA)<sub>2</sub>(PVCL/TA)<sub>4</sub> and (PVCL/TA)<sub>4</sub>(PVCL/PLAA)<sub>4</sub>(PVCL/TA)<sub>4</sub> sandwiched systems. This correlates well with the number of consecutively deposited PVCL/PLAA bilayers, which was 1, 2, and 4 for alternating [(PVCL/TA)<sub>1</sub>(PVCL/PLAA)<sub>1</sub>]<sub>5.5</sub>, (PVCL/TA)<sub>4</sub>(PVCL/PLAA)<sub>2</sub>(PVCL/TA)<sub>4</sub> and (PVCL/TA)<sub>4</sub>(PVCL/PLAA)<sub>4</sub>(PVCL/TA)<sub>4</sub> sandwiched films, respectively. The higher the number of consecutive PVCL/PLAA bilayers, the higher is the local concentration of excess negative charge at a certain pH value, and the lower the critical pH value for PLAA release. Another striking feature in Figure 7 is the difference in the film fractional loss at pH 7.5. A clear transition is observed from the situation when the remaining film components reassociate and remain attached to the substrate after PLAA release (as in the case of (PVCL/TA)<sub>4</sub>(PVCL/PLAA)<sub>2</sub>(PVCL/TA)<sub>4</sub> film), to the situation when dissociation of the PVCL/PLAA middle stack results in release of the top PVCL/TA stack (as in the case of (PVCL/TA)<sub>4</sub>(PVCL/PLAA)<sub>4</sub>(PVCL/TA)<sub>4</sub> film).

In addition to the high osmotic pressure argument, such a transition can also be explained by a decreased proximity between PVCL/TA stacks as the number of spacer PVCL/PLAA layers is increased. A similar dependence of the mode of film release on the number of “weak” polymer pairs for other types of polymer multilayers was also found by Schlenoff and Caruso. Schlenoff et al. reported on selective decomposition of more easily deconstructable polyelectrolyte stacks through changes in pH or salt concentrations. To obtain well-separated free-standing membranes, it was necessary to avoid interpenetration between neighboring “strong” polyelectrolyte strata by deposit-



Scheme 3. Schematic Representation of Film Destruction for Alternating and Stacked Hybrid Multilayers



ing several “weak” bilayers within a decomposable polyelectrolyte stack.<sup>15</sup> In a related study, Caruso and co-workers reported the construction of alternating stacks of electrostatically assembled PAH/PSS and hydrogen-bonded PAA/poly(4-vinylpyridine) (P4VP) to control film destruction properties. They also found that pH-induced film destruction could be achieved through disruption of hydrogen-bonded PAA/P4VP stacks, and the amount of film loss increased with the number of hydrogen-bonded layers inserted between the electrostatically assembled PAH/PSS stacks.<sup>16</sup>

**II.3. TA and PVCL Retained after PLAA Release.** From the ATR-FTIR data, we have also determined the amount of TA and PVCL remaining at the surface after release of PLAA. Since PLAA is completely ionized and released at pH 7.5, the 1716  $\text{cm}^{-1}$  band in the spectra of hybrid TA/PVCL/PLAA multilayers can be assigned solely to the ester carbonyl stretch vibrations of TA and associated with the TA retained within the film. The intensity of this peak was quantified by integration in the region from 1655 to 1770  $\text{cm}^{-1}$  (peak 1 in Supporting Information) and normalized to the absorbance of the same peak at pH 2 after subtracting the contribution of PLAA layers deposited at pH 2. To quantify the amount of PVCL remaining within the film, the intensity of TA at 1600  $\text{cm}^{-1}$  was subtracted from the total intensity at 1600  $\text{cm}^{-1}$  (peak 3 in Supporting Information) and normalized to the initial intensity of PVCL at pH 2.

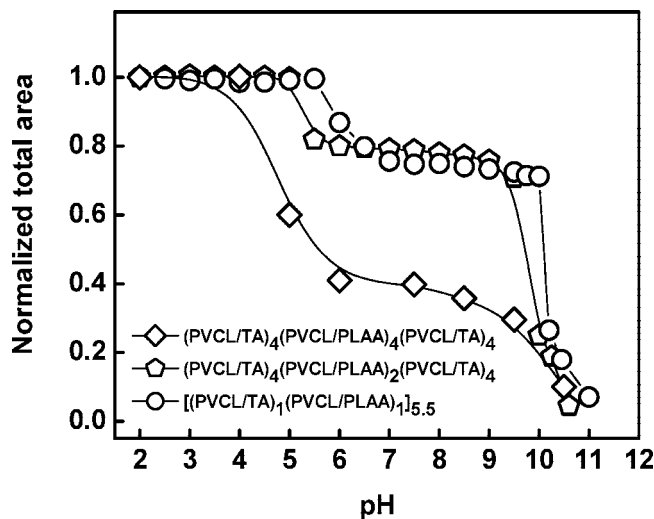


**Figure 7.** pH-triggered disintegration of  $(\text{PVCL}/\text{TA})_4(\text{PVCL}/\text{PLAA})_2(\text{PVCL}/\text{TA})_4$  (pentagons) and  $(\text{PVCL}/\text{TA})_4(\text{PVCL}/\text{PLAA})_4(\text{PVCL}/\text{TA})_4$  (diamonds) sandwiched films deposited at pH 2 in 0.01 M buffered  $\text{D}_2\text{O}$ .  $[(\text{PVCL}/\text{TA})_1(\text{PVCL}/\text{PLAA})_1]_{5.5}$  alternating films (circles) is shown for comparison. Normalized total area in the 1540–1770  $\text{cm}^{-1}$  region is plotted as a function of pH.

Figure 8 contrasts the amounts of TA and PVCL remaining at the surface for films with various layered architecture. The amounts of TA and PVCL retained at the surface were significantly affected by the number of PLAA layers in the middle stack. In the case of  $(\text{PVCL}/\text{PLAA})_6(\text{PVCL}/\text{TA})_6$  stacked

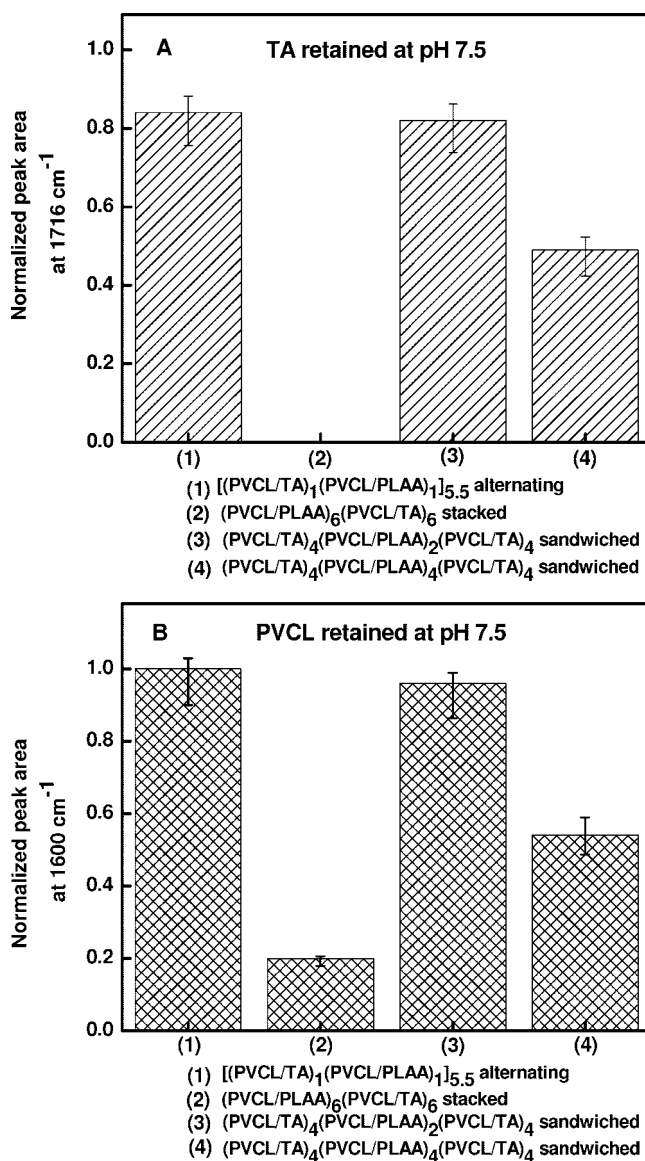


**Figure 8.** TA (panel A) and PVCL (panel B) retained at pH 7.5. All peak intensities were normalized to the corresponding peak intensities at pH 2.

films, almost complete removal of TA and PVCL from the surface was found. A small amount of PVCL remaining is due to the first PVCL layer adsorbed at a substrate. Amounts of TA and PVCL retained for sandwiched (PVCL/TA)<sub>4</sub>(PVCL/PLAA)<sub>4</sub>(PVCL/TA)<sub>4</sub> films were also consistent with the removal of the top PVCL/TA stack. However, for the two systems with a small number of consecutively deposited PVCL/PLAA layers ([ (PVCL/TA)<sub>1</sub>(PVCL/PLAA)<sub>1</sub>]<sub>5.5</sub> alternating and (PVCL/TA)<sub>4</sub>(PVCL/PLAA)<sub>2</sub>(PVCL/TA)<sub>4</sub> sandwiched films), PVCL was almost completely retained at the surface. Surprisingly, we found that diffusion of PLAA through the PVCL/TA in the latter two systems triggered partial (15–20%) desorption of TA from the film. We ascribe the observed triggered desorption to the rigidity and relatively weak (per TA molecule) hydrogen bonding of TA within the film compared to linear polymers. We argue that a rigid TA molecule bound to a PVCL chain through a relatively small number of hydrogen bonds (less than 25) can be detached from PVCL by diffusing PLAA chains. Since water-insoluble complexes occurs in a wide range of TA-to-PVCL compositions in solutions,<sup>27</sup> the remaining PVCL/TA film then readjusts its composition toward higher enrichment with PVCL. In contrast to rigid TA, PVCL chains are longer, more flexible and hydrophobic, and therefore capable of rearranging and reassociating with remaining TA molecules within the film.

## Conclusions

We have demonstrated the possibility of tuning the pH-triggered destruction profile of the greatly pH unstable PVCL/PLAA pair to a neutral pH value through construction of hydrogen-bonded hybrid films with highly pH stable hydrogen-bonded PVCL/TA components. We showed that the deposition of PVCL/TA and PVCL/PLAA pairs within alternating or stacked films drastically changed the critical pH and the release profile of film components from surfaces. In all cases, the presence of the PVCL/TA layers shifted release of PLAA to more basic values in the pH scale. Significantly, alternating TA/PVCL/PLAA films showed the largest pH shift in PLAA release, as well as demonstrated significantly slow release kinetics.

We also show that diffusion of PLAA through the film triggered partial release of TA from the film, and the amounts of all components released from films at a certain pH value were highly affected by film architecture and/or thickness of hydrogen-bonded barrier stacks. The fundamental concept of this work can be applied to other polymer systems containing weakly and strongly dissociating polymer pairs assembled within LbL films. In addition to the possibility of tuning the destruction properties through film architecture, the biocompatibility of film components studied in this paper makes these films potential candidates for future applications in controlled delivery of molecules from surfaces in living systems.

**Acknowledgment.** The authors thank Tom Cattabiani for valuable suggestions. This work was supported by the National Science Foundation (Grant DMR-0710591).

**Supporting Information Available:** Curve-fitting procedure to separate the absorbances of the bands and comparison of ellipsometry and ATR-FTIR results. This material is available free of charge via the Internet at <http://pubs.acs.org>.

## References and Notes

- (1) Shiratori, S. S.; Rubner, M. F. *Macromolecules* **2000**, *33*, 4213.
- (2) Harris, J. J.; Bruening, M. L. *Langmuir* **2000**, *16*, 2006.
- (3) Hiller, J. A.; Rubner, M. F. *Macromolecules* **2003**, *36*, 4078.
- (4) Mendelsohn, J. D.; Barrett, C. J.; Chan, V. V.; Pal, A. J.; Mayes, A. M.; Rubner, M. F. *Langmuir* **2000**, *16*, 16000.
- (5) Fery, A.; Schöler, B.; Cassagneau, T.; Caruso, F. *Langmuir* **2001**, *17*, 3779.
- (6) Hiller, J.; Mendelsohn, J.; Rubner, M. F. *Nat. Mater.* **2002**, *1*, 59.
- (7) Chung, A. J.; Rubner, M. F. *Langmuir* **2002**, *18*, 1176.
- (8) Kharlampieva, E.; Sukhishvili, S. A. *Langmuir* **2004**, *20*, 9677.
- (9) Sui, Z.; Schlenoff, J. B. *Langmuir* **2003**, *19*, 7829.
- (10) Wang, T. C.; Rubner, M. F.; Cohen, R. E. *Langmuir* **2002**, *18*, 3370.
- (11) Hammond, P. T. *Curr. Opin. Colloid Interface Sci.* **2000**, *4*, 430.
- (12) Stockton, W. B.; Rubner, M. F. *Macromolecules* **1997**, *30*, 2717.
- (13) Zhang, H.; Wang, Z.; Zhang, Y.; Zhang, X. *Langmuir* **2004**, *20*, 9366.
- (14) Sukhishvili, S. A.; Granick, S. *J. Am. Chem. Soc.* **2000**, *122*, 9550.
- (15) Dubas, S. T.; Farhat, T. R.; Schlenoff, J. B. *J. Am. Chem. Soc.* **2001**, *123*, 5368.
- (16) Cho, J.; Caruso, F. *Macromolecules* **2003**, *36*, 2845.
- (17) Lavalley, P.; Gergely, C.; Cuisinier, F. J.; Decher, G.; Schaaf, P.; Voegel, J. C.; Picart, C. *Macromolecules* **2002**, *35*, 4458.
- (18) Picart, C.; Mutterer, J.; Richert, L.; Luo, Y.; Prestwich, G. D.; Schaaf, P.; Voegel, J.-C.; Lavalley, P. *PNAS* **2002**, *99*, 12531.
- (19) Sui, Z.; Schlenoff, J. B. *Langmuir* **2004**, *20*, 6026.
- (20) Jomaa, H. W.; Schlenoff, J. B. *Langmuir* **2005**, *21*, 8081.
- (21) Zacharia, N. S.; DeLongchamp, D. M.; Modestino, M.; Hammond, P. T. *Macromolecules* **2007**, *40*, 1598.
- (22) Zacharia, N. S.; Modestino, M.; Hammond, P. T. *Macromolecules* **2007**, *40*, 9523.
- (23) Garza, J. M.; Schaaf, P.; Muller, S.; Ball, V.; Stoltz, J.-F.; Voegel, J.-C.; Lavalley, P. *Langmuir* **2004**, *20*, 7298.
- (24) Vazquez, E.; Dewitt, D. M.; Hammond, P. T.; Lynn, D. M. *J. Am. Chem. Soc.* **2002**, *124*, 13992.
- (25) Wood, K. C.; Boedicker, J. Q.; Lynn, D. M.; Hammond, P. T. *Langmuir* **2005**, *21*, 1603.
- (26) Wood, K. C.; Chuang, H. F.; Batten, R. D.; Lynn, D. M.; Hammond, P. T. *PNAS* **2006**, *103*, 10207.
- (27) Erel-Unal, I.; Sukhishvili, S. A. *Macromolecules* **2008**, *41*, 3962.
- (28) Pristinski, D.; Kozlovskaya, V.; Sukhishvili, S. A. *J. Opt. Soc. Am. A* **2006**, *23*, 2639.
- (29) Kharlampieva, E.; Sukhishvili, S. A. *J. Macromol. Sci., Part C: Polym. Rev.* **2006**, *46*, 1.
- (30) Kharlampieva, E.; Kozlovskaya, V.; Tyutina, J.; Sukhishvili, S. A. *Macromolecules* **2005**, *38*, 10523.
- (31) Bangham, A. D.; Pethica, B. A.; Seaman, G. V. F. *Biochem. J.* **1958**, *69*, 12.
- (32) Jackson, M.; Haris, P. I.; Chapman, D. *Biochim. Biophys. Acta* **1989**, *998*, 75.
- (33) Kharlampieva, E.; Sukhishvili, S. A. *Macromolecules* **2003**, *36*, 9950.
- (34) Kharlampieva, E.; Sukhishvili, S. A. *Langmuir* **2004**, *20*, 10712.
- (35) Mauser, T.; Dejugnat, C.; Mohwald, H.; Sukhorukov, G. B. *Langmuir* **2006**, *22*, 5888.
- (36) Sui, Z.; Schlenoff, J. B. *Langmuir* **2004**, *20*, 6026.
- (37) Decher, G. *Science* **1997**, *277*, 1232.

MA8013564